

# Performance Evaluation of Access Channel Slot Acquisition in Cellular DS/CDMA Reverse Link

Bub-Joo Kang and Youngnam Han

## CONTENTS

- I. INTRODUCTION
- II. SYSTEM DESCRIPTION
- III. ACQUISITION ANALYSIS
- IV. NUMERICAL RESULTS
- V. CONCLUSION
- REFERENCES

## ABSTRACT

In this paper, we consider the acquisition performance of an IS-95 reverse link access channel slot as a function of system design parameters such as postdetection integration length and the number of access channel message block repetitions. The uncertainty region of the reverse link spreading codes compared to that of forward link is very small, since the uncertainty region of the reverse link is determined by a cell radius. Thus, the parallel acquisition technique in the reverse link is more efficient than a serial acquisition technique in terms of implementation and of acquisition time. The parallel acquisition is achieved by a bank of  $N$  parallel I/Q noncoherent correlators. The output characteristics of an I/Q noncoherent correlator are analyzed for band-limited noise and the Rayleigh fast fading channel. The detection probability is derived for multiple correct code-phase offsets and multipath fading. The probability of no message error is derived when rake combining, access channel message block combining, and Viterbi decoding are applied. Numerical results provide the acquisition performance for system design parameters such as postdetection integration length and number of access channel message block repetitions in case of a random access on a mobile station.

## I. INTRODUCTION

In recent years, direct sequence code division multiple access (DS/CDMA) has become more popular in digital cellular and wireless communication networks. There are several advantages that make DS/CDMA an attractive radio access technique. These advantages include the ability to combat multipath and allow multiple users to simultaneously communicate over a channel. However, the advantages of DS/CDMA can be exploited only if the pseudonoise (PN) code sequence of a receiver and an incoming signal are synchronized within a fraction of a PN chip. Typically, the process of synchronization is done in two steps, acquisition (coarse alignment) and tracking (fine alignment) [1], [2]. This paper is mainly focused on the acquisition of the reverse link in the IS-95 CDMA digital cellular system. In the reverse link, since a pilot channel is not utilized in order to conserve mobile station power, noncoherent demodulation is used for the voice/data traffic channel and access channel [3]. In consideration of hardware complexity, I/Q noncoherent correlators are used for acquisition operations as well.

Typically, cells in digital cellular and wireless communication networks are classified roughly according to cell radius as macrocells and microcells. The maximum cell radiuses of macrocells and microcells are 20 km and 1 km, respectively. In case of macrocells, since the propagation delay is about  $3\mu\text{s}/\text{km}$ , the maximum round trip

delay corresponds to about  $120\mu\text{s}$ . When the period of a PN chip,  $T_c$ , is  $1\mu\text{s}$ , the uncertainty region of reverse link is about 120 PN chips. Thus, compared to the uncertainty region of a forward link which is the entire code period (32768 PN chips), that of the reverse link is very small. In case of a small uncertainty region, parallel acquisition is more efficient than serial acquisition in terms of implementation and of acquisition time. Also, a single-dwell detection scheme is known to be more efficient than a multiple-dwell detection scheme over the initial acquisition of a reverse link access channel slot [4].

A parallel acquisition technique that employs a bank of  $N$  parallel I/Q noncoherent matched filters (MFs) is discussed in [5], [6]. In this paper, we consider correlators rather than matched filters. The output characteristic of an I/Q noncoherent correlator is analyzed for the band-limited and Rayleigh fast fading channel. The independent fading of all users is assumed. The detection probability is derived for multiple  $H_1$  hypotheses and multipath fading [4]. The probability of no message error is derived when rake combining, access channel message block combining, and Viterbi decoding are applied. Based on these evaluations, suboptimum values of system design parameters such as postdetection integration length (noncoherent summations) and the number of access channel message block repetitions are chosen in terms of mean acquisition time and mean slot acquisition

time. These values are also chosen for cases without antenna diversity and with antenna diversity.

This paper is organized as follows. The procedure of random access and slot acquisition is described in Section II. The output characteristic of an I/Q noncoherent correlator, mean slot acquisition time, and required probability are analyzed in Section III. Numerical results are presented in Section IV, and finally, a concluding discussion is presented in Section V.

## II. SYSTEM DESCRIPTION

The DS/CDMA reverse link consists of the access and reverse traffic channels [7]. The access channel is used for a random access, while the reverse traffic channel is used for communicating user traffic data. When a mobile station attempts to access a network, an access channel slot (pseudorandomly selected transmission time interval) is utilized. Transmissions during an access channel slot consist an access channel preamble unmodulated by data and an access channel message capsule consisting of access messages encoded for error detection with a cyclic redundancy code (CRC). In order to analyze the acquisition performance of access channel slot transmissions, the following assumptions are made :

- 1) The access channel transmission uses 9600 bps mode.
- 2) An access channel message block is defined as the result that an access channel message is convolutionally encoded.
- 3) An access channel message capsule consists of several access channel message blocks.

The random access procedure is briefly described. The transmission timing of an access channel slot is determined pseudorandomly. If the initial acquisition is achieved during a given access channel preamble, the base station proceeds with noncoherent demodulation of M-ary orthogonal signals, Viterbi decoding, and CRC checking over the succeeding access channel message capsule. If no error is detected by CRC checking, the access attempt succeeds tentatively, and the base station sends an acknowledgment to the mobile station. If an acknowledgment is correctly received, an access attempt terminates. But, if errors are detected by CRC checking, the access attempt fails, and the base station does not send an acknowledgment to the mobile station. In case of an access attempt failure, the access channel slot is pseudorandomly repeated at the base of the system time, namely, it is retransmitted a random delay whose average corresponds to several slots.

In the reverse link, since the transmitted signal of a mobile station is always spread by the PN code sequence with zero code-phase offset, the uncertainty region is determined by the round-trip delay due to the cell radius. Thus, the uncertainty region,  $V$ , can be represented as  $W/\Delta$ , where

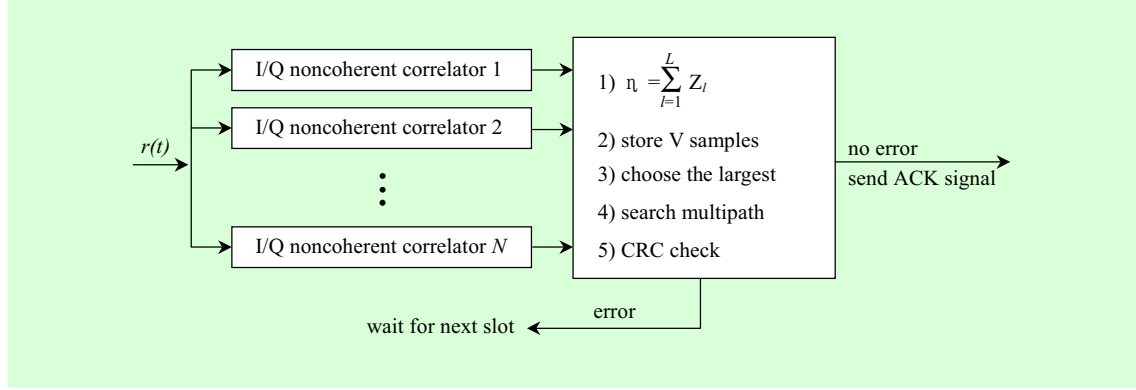


Fig. 10. System structure.

$W$  and  $\Delta$  are the number of PN chips for round-trip delay and search step size, respectively.

The acquisition system under consideration in this paper is a parallel acquisition using a single-dwell detection scheme. Since the parallel acquisition is done by a bank of  $N$  parallel I/Q noncoherent correlators as shown in Fig. 1, the number of total test hypotheses for each I/Q noncoherent correlator is given by  $V/N$ . The parallel acquisition algorithm using single-dwell detection is as follows : Defining the sample as the sum  $\eta$  of I/Q noncoherent correlator outputs for the postdetection integration (noncoherent summations) length  $L$  as shown in Fig. 1, the samples corresponding to all test hypotheses are compared. Finally, this scheme only chooses the test hypothesis (code-phase offset) that corresponds to the largest one among  $V$  samples. After completing this procedure, the multipath acquisition is done over  $\pm W_p$  chips

range centered on the code-phase that is already selected.  $W_p$  is  $\lfloor T_m/T_c \rfloor + 1$ , where  $T_m$  is the delay spread of a channel,  $T_c$  is the period of a PN chip, and  $\lfloor \cdot \rfloor$  denotes the integer part. This selects the other code-phase offset that corresponds to the largest sample except the code-phase offset that is already selected. Thus, the initial acquisition is terminated by finishing the multipath search.

### III. ACQUISITION ANALYSIS

#### 1. Output Characteristic of I/Q Noncoherent Correlator

In order to evaluate the acquisition performance, we consider the discrete multipath Rayleigh fading channel [10]. The discrete multipath intensity profile  $\rho(\tau)$  of a fading channel as a function of the time delay  $\tau$  can be modeled by

$$\rho(\tau) = \sum_{i=1}^J E[\alpha_i^2] \delta(\tau - \tau_i), \quad (1)$$

where  $\alpha_i$  and  $\tau_i$  are the path gain and time delay of the  $i$ -th path, respectively. The path gains are independent, identically distributed, Rayleigh random variables with mean square values  $E[\alpha_i^2]$ . The number of multipath components,  $J$ , is  $\lfloor T_m/T_c \rfloor + 1$ . In IS-95 [7], the transmitted access channel preamble of the  $k$ -th user can be represented as

$$S^{(k)}(t) = \sqrt{E_c^{(k)}} \cos \omega_c(t) \sum_n w_{0,n}^{(k)} a_{I,n}^{(k)} h(t - nT_c) \\ + \sqrt{E_c^{(k)}} \sin \omega_c(t) \sum_n w_{0,n}^{(k)} a_{Q,n}^{(k)} h(t - nT_c), \quad (2)$$

where  $a_{I,n}^{(k)}$ ,  $a_{Q,n}^{(k)}$  are the I and Q PN sequences, respectively,  $w_{0,n}^{(k)}$  is the Walsh index 0 sequence,  $E_c^{(k)}$  is the PN chip energy, and  $h(t)$  is the impulse response of a band-limited filter.

In the presence of noise with multipath and of other users from the same and other cells in the reverse link, the received signal in cellular DS/CDMA reverse link can be written as

$$r(t) = \sum_{i=1}^{N_u} \sum_{j=1}^J \alpha_j^{(i)} \sqrt{E_c^{(i)}} \left[ \cos(\omega_c t - \varphi_j^{(i)}) \cdot \sum_n w_{s,n}^{(i)} a_{I,n}^{(i)} h(t - nT_c - \tau_j^{(i)}) + \sin(\omega_c t - \varphi_j^{(i)}) \cdot \sum_n w_{s,n}^{(i)} a_{Q,n}^{(i)} h(t - nT_c - \tau_j^{(i)}) \right] \\ + \sum_{m=1}^{N_c} \sum_{i=1}^{N_u} \sum_{j=1}^J \alpha_j^{(mi)} \sqrt{E_c^{(mi)}} \left[ \cos(\omega_c t - \varphi_j^{(mi)}) \cdot \sum_n w_{s,n}^{(mi)} a_{I,n}^{(mi)} h(t - nT_c - \tau_j^{(mi)}) + \sin(\omega_c t - \varphi_j^{(mi)}) \cdot \sum_n w_{s,n}^{(mi)} a_{Q,n}^{(mi)} h(t - nT_c - \tau_j^{(mi)}) \right] + n(t) \quad (3)$$

where  $N_u$  and  $N_c$  are the number of users and the number of other cells, respectively,

$\varphi_j^{(i)}$  is the random phase of the  $j$ -th path for the  $i$ -th user,  $w_{s,n}^{(i)}$  is the Walsh index  $s$  sequence of the  $i$ -th user, and  $n(t)$  is an additive white Gaussian random process with zero mean and two-sided power spectral density  $N_0/2$ . Also, the subscript  $m$  denotes the other cell component.

Referring to (3) and I/Q noncoherent correlator of Fig. 2,  $Y_I$  and  $Y_Q$  for the  $h$ -th path of the  $k$ -th user in the home cell can be represented as

$$Y_I = N_w \sqrt{E_c^{(k)}} \sum_{j=1}^J \alpha_j^{(k)} R(\lambda_h^{(j)}) \cos \varphi_j^{(k)} + \sum_{n=1}^{N_w} n_{I,n} \quad (4)$$

and

$$Y_Q = N_w \sqrt{E_c^{(k)}} \sum_{j=1}^J \alpha_j^{(k)} R(\lambda_h^{(j)}) \sin \varphi_j^{(k)} + \sum_{n=1}^{N_w} n_{Q,n}, \quad (5)$$

where  $R(\lambda_h^{(j)}) = \int |H(f)|^2 \cos(2\pi f \lambda_h^{(j)}) df$ ,  $\lambda_h^{(j)}$  is the timing error between the  $j$ -th path and PN code sequence of local PN code generator corresponding to the  $h$ -th path,  $N_w$  is the number of PN chips for a Walsh symbol duration.

The variance consists of the contribution from background noise, multipath interference, multiple access interference, and other cell interference. From (4) and (5), the variance of  $Y_I$  and  $Y_Q$  is given by

$$\text{Var}[Y_I] = \text{Var}[Y_Q] = \sigma_1^2, \quad (6)$$

where  $\sigma_1^2$  is the interference variance for the  $h$ -path of the  $k$ -th user.

To evaluate the interference variance on the reverse link, we assume that the number of users is the same in all cells and users

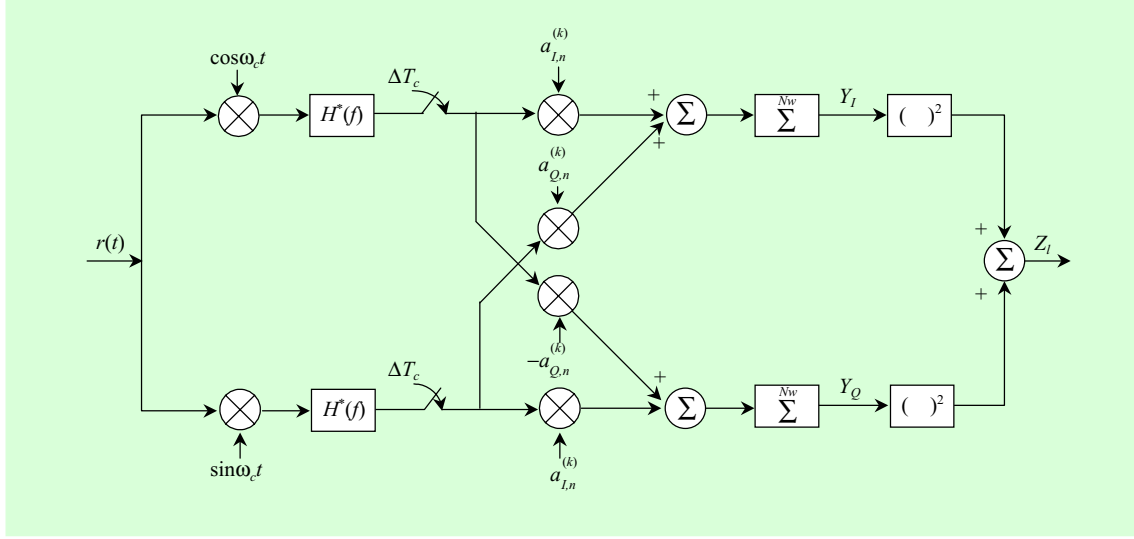


Fig. 11. I/Q noncoherent correlator.

are uniformly distributed. Also, the fading of all users in all cells is assumed to be independent. In general, the interference described above is treated as an additive Gaussian noise. In this case, under hypothesis  $H_1$  corresponding to the  $h$ -th path of the  $k$ -th user, the interference variance  $\sigma_1^2$  can be represented as

$$\sigma_1^2 = \frac{N_w}{2} \left[ N_0 + E_c^{(k)} E\{(\alpha_h^{(k)})^2\} \sum_{\substack{n=-\infty \\ n \neq 0}}^{\infty} [R(nT_c + \lambda_h^{(h)})]^2 \right. \\ + E_c^{(k)} \sum_{\substack{j=1 \\ j \neq h}}^J E\{(\alpha_j^{(k)})^2\} \sum_{n=-\infty}^{\infty} [R(nT_c + \lambda_h^{(j)})]^2 \\ + \sum_{\substack{i=1 \\ i \neq k}}^{N_u} E_c^{(i)} \sum_{j=1}^J E\{(\alpha_j^{(i)})^2\} \sum_{n=-\infty}^{\infty} [R(nT_c + \lambda_h^{(ij)})]^2 \\ \left. + R_f \sum_{i=1}^{N_u} E_c^{(i)} \sum_{j=1}^J E\{(\alpha_j^{(i)})^2\} \sum_{n=-\infty}^{\infty} [R(nT_c + \lambda_h^{(ij)})]^2 \right] \quad (7)$$

where  $\lambda_h^{(j)}$  is the timing difference between the  $h$ -th path and the  $j$ -th path of the  $k$ -th

user,  $\lambda_h^{(ij)}$  is the timing difference between the  $h$ -th path of the  $k$ -th user and the  $j$ -th path of the  $i$ -th user, and  $R_f$  is the ratio of total other cell user interference to home cell other user interference. Typical value for  $R_f$  is 0.55 [8]. In (7), the first term is background noise component, the second term is the intersymbol interference component, the third term is the multipath interference component, the fourth and fifth terms are the other user interference components of home cell and of other cells, respectively.

Then, if we assume that the number of users is the same in all cells and users are uniformly distributed, the interference variance  $\sigma_1^2$  for the  $h$ -th path of the  $k$ -th user can be rewritten as

$$\sigma_1^2 = \frac{N_w}{2} \left[ N_0 + E_c E\{\alpha_h^2\} \sum_{\substack{n=-\infty \\ n \neq 0}}^{\infty} [R(nT_c + \lambda_h^{(h)})]^2 \right]$$

$$\begin{aligned}
& + E_c \sum_{\substack{j=1 \\ j \neq h}}^J E\{\alpha_j^2\} \sum_{n=-\infty}^{\infty} [R(nT_c + \lambda_h^{(j)})]^2 \\
& + \{(N_u - 1) + R_f N_u\} E_c \sum_{j=1}^J E\{\alpha_j^2\} \\
& \cdot \sum_{n=-\infty}^{\infty} [R(nT_c)]^2 \Bigg], \quad (8)
\end{aligned}$$

where  $\sigma_1^2$  is also based on an implicit assumption that the phase  $\varphi_j^{(k)}$  in (4) and (5) remains constant over the  $N_w$  PN chips accumulated.

Also, the variance  $\sigma_0^2$  of  $Y_I$  and  $Y_Q$  under hypothesis  $H_0$  (incorrect acquisition case) can be represented as

$$\begin{aligned}
\sigma_0^2 = & \frac{N_w}{2} \left[ N_0 + N_u(1 + R_f) E_c \sum_{j=1}^J E\{\alpha_j^2\} \right. \\
& \cdot \left. \sum_{n=-\infty}^{\infty} [R(nT_c)]^2 \right]. \quad (9)
\end{aligned}$$

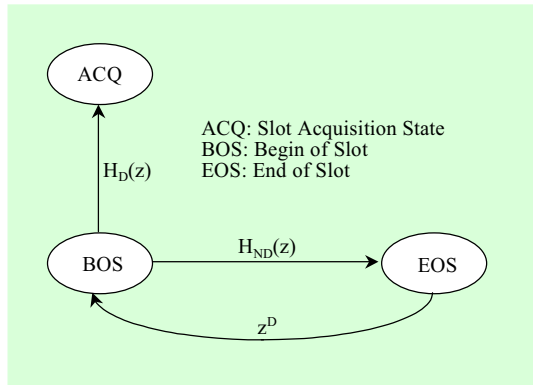


**Fig. 12.** State diagram of the access channel slot acquisition.

## 2. Mean Slot Acquisition Time

State diagram is used to derive the probability generating function of acquisition

time owing to Markovian nature of the acquisition process. The state diagram of access channel slot acquisition described in Section II is shown in Fig. 3.  $H_D(z)$  and  $H_{ND}(z)$  of Fig. 3 are given by

$$H_D(z) = P_D P_C z^S \quad (10)$$

and

$$H_{HD}(z) = (1 - P_D P_C) z^S, \quad (11)$$

where  $P_D$  and  $P_C$  are the detection probability and probability of no message error, respectively.  $S$  is the size of access channel slot comprised of access channel preamble and access channel message capsule. From Fig. 3, the generating function is

$$U(z) = \frac{H_D(z)}{1 - z^D H_{ND}(z)}, \quad (12)$$

where  $D$  is the average random-delay. Thus, the mean slot acquisition time,  $E[T_{ACQ}]$ , is given by

$$\begin{aligned}
E[T_{ACQ}] &= \left. \frac{d}{dz} \ln U(z) \right|_{z=1} \\
&= \frac{S + D(1 - P_D P_C)}{P_D P_C}. \quad (13)
\end{aligned}$$

## 3. Detection Probability and Probability of No Message Error

To facilitate the derivation of detection probability, we made the following assumptions : 1) all test statistics are independent, 2) there are  $IH_1$  cells in the uncertainty region, 3) all test cells are a priori equally likely, and 4) the output characteristic of an I/Q noncoherent correlator is analyzed for the fast fading model

with Rayleigh-distributed envelope statistics. If the decision variable  $\eta$  is the sum of I/Q noncoherent correlator outputs  $Z_l$ ,  $l = 1, 2, \dots, L$ , which are mutually independent,  $\eta$  under the hypothesis  $H_0$  is central chi-square distributed with  $2L$  degrees of freedom. Hence, the probability density function of  $\eta$  under the hypothesis  $H_0$  is given by

$$f_\eta(\eta|H_0) = \frac{1}{(L-1)!V_N^L} \eta^{L-1} e^{-\frac{\eta}{V_N}}, \quad (14)$$

where  $V_N = 2\sigma_0^2 = N_w I_0$ , and  $I_0$  is the interference density under hypothesis  $H_0$ .

From (4) and (5), the I/Q noncoherent correlator output means  $V_{F_i}$ ,  $i = 1, 2, \dots, I$  under the hypothesis  $H_1$  are given by

$$V_{F_i} = N_w^2 E_c \sum_{j=1}^J E\{\alpha_j^2\} [R(\lambda_i^{(j)})^2 + 2\sigma_1^2],$$

$$i = 1, 2, \dots, I, \quad (15)$$

where  $R(\lambda_i^{(j)}) = \int |H(f)|^2 \cos(2\pi f \lambda_i^{(j)}) df$ ,  $\alpha_j$  is the path gain of the  $j$ -th path,  $\lambda_i^{(j)}$  is the timing error between the  $j$ -th path and code sequence of local PN code generator corresponding to the  $H_{1i}$  cell, and  $N_w I_0 = 2\sigma_1^2$ . Using (15), the probability density function of  $\eta$  under the hypothesis  $H_1$  is given by

$$f_\eta(\eta|H_{1i}) = \frac{1}{(L-1)!V_{F_i}^L} \eta^{L-1} e^{-\frac{\eta}{V_{F_i}}},$$

$$i = 1, 2, \dots, I. \quad (16)$$

Using the probability density functions of (14) and (16) above, the detection probability can be derived. Since the detection probability  $P_{D_{1i}}$  corresponding to the  $H_{1i}$  cell is the probability that the  $H_{1i}$  is larger

than  $(V-1)$  cells, the detection probability  $P_{D_{1i}}$  is represented as

$$P_{D_{1i}} = \int_0^\infty f_\eta(\eta|H_{1i}) \left[ \int_0^\eta f_x(x|H_0) dx \right]^{(V-1)} \cdot \prod_{\substack{l=1 \\ l \neq i}}^I \left[ \int_0^\eta f_y(y|H_{1l}) dy \right] d\eta. \quad (17)$$

Since there are  $IH_1$  cells in the uncertainty region, the detection probability  $P_D$  is given by

$$P_D = \sum_{i=1}^I P_{D_{1i}}. \quad (18)$$

The probability of no message error  $P_C$  is the probability that no error is detected within an access channel message block,  $B_L$ . After CRC checking, it is given by [11]

$$P_C = (1 - P_B)^{B_L}, \quad (19)$$

where  $P_B$  is the bit error probability after the hard-decision Viterbi decoding. Then,  $P_B$  is upper bounded by

$$P_B \leq \frac{1}{2} \frac{dT(D, N)}{dN} \Big|_{N=1, D=\sqrt{4\varepsilon(1-\varepsilon)}}, \quad (20)$$

where  $\varepsilon$  is the bit error probability of M-ary orthogonal signals for the multipath Rayleigh fading channel. We assume that a received access channel message block experiences independent fading. Under these fading environments, the symbol error probability of M-ary orthogonal signals for  $T(\leq J)$  path combining and  $N_r$  access channel message block combining is given by [10]

$$P_M = 1 - \int_0^\infty \frac{z^{R-1} e^{-z/(1+\bar{r}_c)}}{(R-1)!(1+\bar{r}_c)^R} \cdot \left[ 1 - e^{-z/V_N} \sum_{k=0}^{R-1} \frac{(z/V_N)^k}{k!} \right]^{M-1} dz, \quad (21)$$

where  $R = TN_r$ ,  $\bar{r}_c = \frac{1}{R} \sum_{j=1}^R E[\alpha_j^2] N_w E_c$ .

Thus, the bit error probability of M-ary orthogonal signals is given by

$$\varepsilon = \frac{M/2}{M-1} P_M. \quad (22)$$

#### IV. NUMERICAL RESULTS

To evaluate the acquisition performance, we consider the following parameters : the period of a PN chip  $T_c=813.8$  ns, number of PN chips per Walsh symbol duration  $N_w=256$ , number of I/Q noncoherent correlators  $N=6$ , number of rake combining paths  $T=4$ , total search window length  $W=148$  PN chips (cell radius = 20 km), multipath search region  $W_p=6$  PN chips, search step size  $\Delta=1/2$ , reset time  $T_r=1.25$  ms, average random-delay  $D=760$  ms, number of Walsh functions  $M=64$ , access channel message block  $B_L=552$  bits.

The average path powers  $E[\alpha_i^2]$ ,  $i = 1, 2, \dots, 6$  of the discrete multipath intensity profile considered in this work are given by 0.5562, 0.2493, 0.1118, 0.0501, and 0.0101, respectively. In order to calculate the bit error probability  $P_B$  given in (18),

$$\left. \frac{dT(D, N)}{dN} \right|_{N=1} \text{ of}$$

the best (3,1,9) convolutional code in (20) is given by [9]

$$\begin{aligned} \left. \frac{dT(D, N)}{dN} \right|_{N=1} = & 11D^{18} + 32D^{20} + 195D^{22} \\ & + 564D^{24} + 1473D^{26} + 5129D^{28} \\ & + 17434D^{30} + 54092D^{32} \\ & + 17117D^{34} + \dots \end{aligned} \quad (23)$$

In this paper, we intend to choose the suboptimum system design parameters of postdetection integration length  $L$  and the number of access channel message block repetitions  $N_r$  in terms of acquisition time and its sensitivity.

From (13), we can calculate the mean acquisition time when  $P_C = 1$ . Figures 4 and 5 show the mean acquisition times in terms of  $E_s/I_0$  in various values of  $L$  for both cases without antenna diversity and with antenna diversity, respectively. Here,  $E_s$  is  $N_w E_c$  and  $I_0$  is the interference spectral density that is represented as  $2\sigma_1^2/N_w$  under hypothesis  $H_1$  and  $2\sigma_0^2/N_w$  under hypothesis  $H_0$ , respectively. In view of the mean acquisition time and its sensitivity to changes in  $E_s/I_0$ , better performances for both cases are achieved when  $L=3$  and  $L=2$ , respectively.

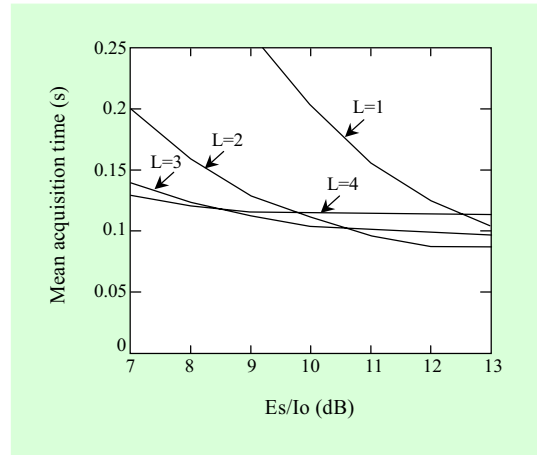


Fig. 13. Mean acquisition time for no antenna diversity.

Figures 6 and 7 show the mean slot acquisition time versus  $E_s/I_0$  for the case

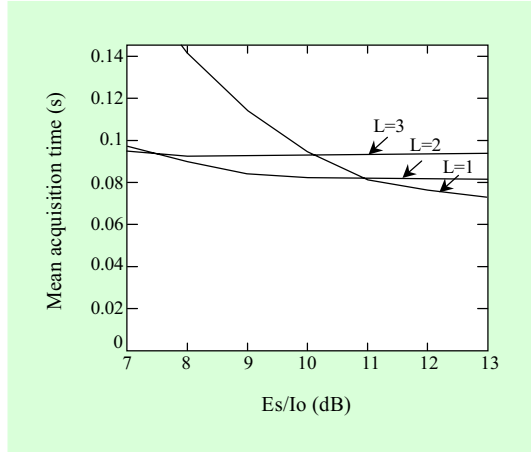


Fig. 14. Mean acquisition time for antenna diversity.

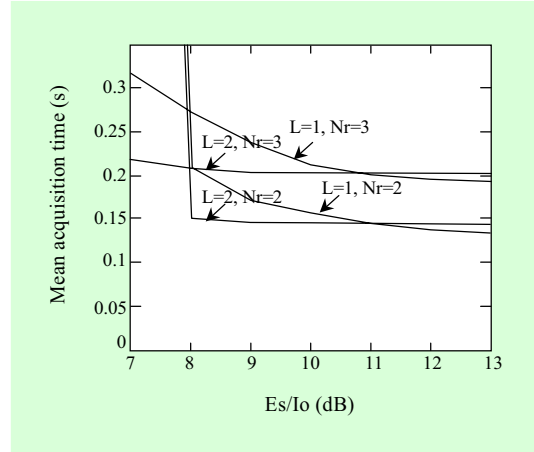


Fig. 16. Mean slot acquisition time for antenna diversity.

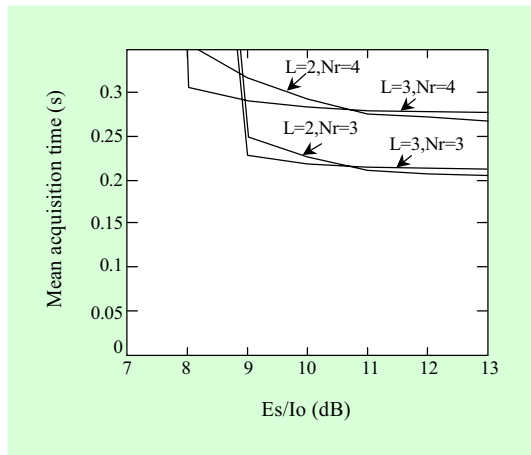


Fig. 15. Mean slot acquisition time for no antenna diversity.

without antenna diversity and the case with antenna diversity. From the results of two figures, the suboptimum choice of the case without antenna diversity is  $L=3$  and  $N_r=4$ , while in the case with antenna diversity, the suboptimum system design parameters are  $L=2$  and  $N_r=2$ . From these suboptimum system design parameters, the

mean acquisition times of both cases are about 0.1 s and 0.08 s, respectively, while the mean slot acquisition times are about 0.3 s and 0.15 s, respectively. Hence, the case with antenna diversity provides two times shorter mean slot acquisition time than the case without antenna diversity. If we also see the sensitivity of mean slot acquisition time with respect to  $L$  and  $N_r$ , its sensitivity to changes in  $L$  is small more or less, but that to changes in  $N_r$  is very large. Hence, the mean slot acquisition time is influenced by the probability of no message error more than the detection probability.

## V. CONCLUSION

The performance of an access channel slot acquisition scheme has been evaluated in terms of mean acquisition time and mean

slot acquisition time, where the parallel acquisition using the single-dwell detection scheme is applied. Comparing the mean slot acquisition time of both cases without antenna diversity and with antenna diversity, the case with antenna diversity can achieve two times shorter acquisition time than the case without antenna diversity. The suboptimum system design parameters such as  $L$  and  $N_r$  have also been suggested for both cases without antenna diversity and with antenna diversity, respectively. In view of the mean slot acquisition time and its sensitivity to changes in  $E_s/I_0$ , the case with antenna diversity performs better when  $L=3$  and  $N_r=4$ , while the case with antenna diversity does better when  $L=2$  and  $N_r=2$ .

## REFERENCES

- [1] A. Polydoros and C. L. Weber, "A Unified Approach to Serial Search Spread-Spectrum Code Acquisition - Part I: General Theory," *IEEE Trans. Commun.*, Vol. Com-32, May 1984, pp. 542-549.
- [2] A. Polydoros and C. L. Weber, "A Unified Approach to Serial Search Spread-Spectrum Code Acquisition - Part II: A Matched-Filter Receiver," *IEEE Trans. Commun.*, Vol. Com-32, May 1984, pp. 550-560.
- [3] K. S. Gilhousen, I. M. Jacobs, R. Padovani, A. J. Viterbi, L. A. Weaver, and C. E. Wheatley, "On the Capacity of a Cellular CDMA System," *IEEE Trans. Vehic. Technol.*, Vol. VT-40, May 1991, pp. 303-312.
- [4] B. J. Kang, H. R. Park, C. E. Kang, and J. Y. Son, "Performance Evaluation of Parallel Acquisition in Cellular DS/CDMA Reverse Link," *IEICE Trans. Commun.*, Vol. E79-B, Sep. 1996, pp. 1301-1308.
- [5] E. A. Sourour and S. C. Gupta, "Direct Sequence Spread Spectrum Parallel Acquisition in a Fading Mobile Channel," *IEEE Trans. Commun.*, Vol. Com-38, July 1990, pp. 992-998.
- [6] E. A. Sourour and S. C. Gupta, "Direct Sequence Spread Spectrum Parallel Acquisition in Nonselective and Frequency-Selective Rician Fading Channels," *IEEE J. Select. Areas in Commun.*, Vol. SAC-10, Apr. 1992, pp. 535-544.
- [7] *TIA/EIA IS-95 Interim standard*, TIA, July 1993.
- [8] A.J. Viterbi, *CDMA Principles of Spread Spectrum Communication*, Addison-Wesley, New York, 1995.
- [9] J. Conan, "The Weight Spectra of Some Short Low-Rate Convolutional Codes," *IEEE Trans. Commun.* Vol. Com-32, pp. 1050-1053, Sep. 1984.
- [10] J.G. Proakis, *Digital communications*, McGraw-Hill, New York, 1989.
- [11] S. Lin, D.J. Costello, Jr., *Error Control Coding: Fundamentals and Applications*, Prentice-Hall, New Jersey, 1983.
- [12] B.J. Kang *et al.*, "Access Channel Slot Acquisition in Cellular DS/CDMA Reverse Link," in *Proc. IEEE VTC'96*, Atlanta, Apr. 1996, pp. 1453-1457.

**Bub-Joo Kang** received the B.S. degree in electronic engineering from Kyunghee University, Seoul, Korea in 1983, and the M.S. and Ph. D. degrees in electronic engineering from Yonsei University, Seoul, Korea in 1985 and 1996, respectively. Since February 1988, he has been working as a senior research engineer at the Mobile Communication Research Division, ETRI, Taejon, Korea. From 1993 to 1995, he worked on the design of demodulator

and Viterbi decoder in DS/CDMA systems. He is currently working on the radio interface design and its performance evaluation in IMT-2000. His current research interests include modulation/demodulation, channel coding, packet radio, CDMA mobile communications, etc.

**Youngnam Han** received his B.S. and M.S. degrees in electrical engineering from Seoul National University in 1978 and 1980, respectively. He received his Ph.D. degree from the University of Massachusetts, Amherst, in 1992. From 1980 to 1983, he served as a full time lecturer at the Korean Naval Academy. Also, during that period, he joined the research team for the under-water vehicle simulator at Agency for Defense Development. From 1983 to 1985, He was with the Kumoh Institute of Technology as a faculty member in the Department of Control Engineering. He also worked for ETRI from 1992 to 1997 and served as a section head in Mobile Telecommunication Division, managing the project of design and performance analysis of radio transmission technology for DCN, PCS and IMT-2000. He is currently an assistant professor in School of Communications Engineering, Information and Communications University, Taejon, Korea. His research interests include performance evaluation of mobile communication systems, optimization of handover algorithms, multiple access technology, and wireless ATM.